

Beamforming Saturation in Two-Timescale RIS-assisted Communication

Masoud Sadeghian*, Angel Lozano*, and Gabor Fodor†‡

*Department of Engineering, Universitat Pompeu Fabra, Barcelona, Spain

†School of Electrical Engineering and Computer Science, KTH Royal Institute of Technology, Stockholm, Sweden

‡Ericsson Research, Sweden

{masoud.sadeghian, angel.lozano}@upf.edu, gaborf@kth.se

Abstract—This paper considers wireless communication assisted by a reconfigurable intelligent surface (RIS), focusing on the two-timescale approach, in which the RIS phase shifts are optimized based on channel statistics to mitigate the overheads associated with channel estimation. It is shown that, while the power captured by the RIS scales linearly with the number of its elements, the two-timescale beamforming gain upon re-radiation towards the receiver saturates rapidly as the number of RIS elements increases, for a broad class of power angular spectra (PAS). The ultimate achievable gain is determined by the decay rate of the PAS in the angular domain, which directly influences how rapidly spatial correlations between RIS elements diminish. The implications of this saturation on the effectiveness of RIS-assisted communications are discussed.

I. INTRODUCTION

Reconfigurable intelligence surfaces (RISs) enable creating smart radio environments in which the propagation is controlled by integrated electronic circuits and software [1]. Since RISs can be built by predominantly passive elements, their deployment appears as an energy and cost efficient complement to large-scale wireless infrastructures, particularly to overcome blockages [2, 3].

Relying on passive phase-shift elements that are devoid of signal processing capabilities implies that estimating both the transmitter-RIS and the RIS-receiver links becomes critical [4, 5]. Indeed, channel estimation in RIS-assisted wireless networks is more challenging than in conventional systems [5]. An approach to circumvent these hurdles is to optimize the phase shifts based on only the channel statistics, rather than its realizations. Sometimes referred to as a two-timescale scheme [6–9], this only requires that the receiver estimates—for coherent detection purposes—the cascade channel connecting it with the transmitter via the RIS. Put differently, the RIS becomes transparent as far as channel estimation is concerned. This is attractive, since standardized sophisticated channel acquisition procedures are supported in contemporary wireless networks.

In this paper, we consider the uplink of a RIS-aided cell in which the base station (BS) is equipped with multiple antennas, and ask the question of how the contribution of the RIS depends on the number of elements it features in a two-timescale scenario. This contribution depends on the amount of power captured by the RIS, and on its beamforming gain when

re-radiating such power towards the receiver. To address this question, an analytical expression is derived for the signal-to-noise ratio (SNR) with optimum reception at the BS when the RIS phase shifts are configured based on the correlation among its elements. These correlations are determined by the topology of the RIS and by the channel’s power angular spectrum (PAS).

The main result of the paper is that, for a linear RIS and a large class of PAS functions that includes those most commonly used to model multipath propagation, the two-timescale RIS beamforming gain saturates as the number of elements grows large. The highest attainable gain depends on how rapidly the PAS decays angularly or, equivalently, on how rapidly the correlations decay over space.

II. SYSTEM MODEL

A single-antenna mobile station (MS) communicates with an N_b -antenna BS, aided by a uniform linear RIS equipped with N_r elements. Since empirical measurements indicate that the elevation angle plays a secondary role in most outdoor deployments [10, Ch. 3], the RIS is horizontally disposed and the formulation involves only the azimuth.

A. Cascade Channel Model

The normalized channel between the BS and the RIS, deterministic and of unit rank, is $\mathbf{H} \in \mathbb{C}^{N_b \times N_r}$ given by

$$\mathbf{H} = \mathbf{a}_b \mathbf{a}_r^*, \quad (1)$$

where \mathbf{a}_b and \mathbf{a}_r are the respective steering vectors at BS and RIS. Precisely, \mathbf{a}_b is an arbitrary steering vector that depends on the topology of the BS and the angle of arrival thereon, while \mathbf{a}_r is a steering vector whose m th entry is

$$[\mathbf{a}_r]_m = \exp\left(j2\pi \frac{md \cos \theta_r}{\lambda_c}\right) \quad m = 0, \dots, N_r - 1, \quad (2)$$

where θ_r is the angle of departure relative to the linear RIS, d is the spacing between RIS elements, and λ_c is the carrier wavelength.

The normalized channel between the MS and the RIS, in turn, is $\mathbf{h}_r \sim \mathcal{N}_{\mathbb{C}}(\mathbf{0}, \mathbf{C}_r)$ with covariance matrix $\mathbf{C}_r \in \mathbb{C}^{N_r \times N_r}$. As it models the multipath portion of the channel, \mathbf{C}_r is nonsingular and, owing to the linear and uniform structure

of the RIS, it exhibits a Toeplitz structure; its (k, ℓ) th entry depends only on $k - \ell = n$, being given by

$$c_n = \int_0^\pi \mathcal{P}(\theta) e^{j2\pi \frac{n d \cos \theta}{\lambda_c}} d\theta \quad (3)$$

for $n = 0, \dots, N_r - 1$, with $\mathcal{P}(\theta)$ the PAS normalized so it can be interpreted as a probability density function [10, Ch. 3] supported on $[0, \pi]$, which corresponds to the half-space facing the RIS. It follows from this PAS normalization that the entries of \mathbf{h}_r are of unit variance, and that $c_0 = 1$ while $c_{-n} = c_n^*$.

With the configuration of the RIS specified by the phase-shift matrix $\Psi = \text{diag}(\psi)$ where $\psi = [e^{-j\psi_0}, \dots, e^{-j\psi_{N_r-1}}]^T$, the cascade channel at the BS from the MS is

$$\mathbf{h} = \mathbf{H}\Psi\mathbf{h}_r. \quad (4)$$

With a statistical optimization of Ψ , the cascade channel satisfies $\mathbf{h} \sim \mathcal{N}_C(\mathbf{0}, \mathbf{C})$ with

$$\mathbf{C} = \mathbf{H}\Psi\mathbf{C}_r\Psi^*\mathbf{H}^*, \quad (5)$$

which is singular on account of the rank-1 nature of \mathbf{H} , and therefore of \mathbf{h} .

While, as mentioned, the estimation of the channels to/from the RIS is utterly challenging, estimating the cascade channel \mathbf{h} at the BS is a standard procedure. In the case at hand, a single pilot symbol transmission suffices. By suitably repeating or power-boosting such pilot transmission, an arbitrarily precise estimate of \mathbf{h} can be procured [11]. Accordingly, perfect knowledge of \mathbf{h} at the BS is considered in the sequel, yet the findings in the paper continue to apply in the face of channel estimation errors; they are merely obscured by the more involved formulation.

B. Uplink Data Signal Model

Upon uplink data transmission, the observation at the BS is

$$\mathbf{y} = \sqrt{\alpha}\mathbf{h}x + \mathbf{n}, \quad (6)$$

where α is the large-scale channel gain, $\mathbf{n} \sim \mathcal{N}_C(\mathbf{0}, \sigma^2 \mathbf{I}_{N_b})$ is the additive white Gaussian noise, and x is a data symbol of power P .

III. AVERAGE SNR IN TWO-TIMESCALE RIS-ASSISTED COMMUNICATION

With \mathbf{h} perfectly known by the BS, the optimum receiver thereon is a linear combiner $\mathbf{w} \in \mathbb{C}^{N_b \times 1}$ satisfying [10]

$$\mathbf{w} \propto \mathbf{h} \quad (7)$$

and the ensuing SNR, for a given \mathbf{h} , equals

$$\text{SNR} = \frac{\mathbb{E}[|\mathbf{w}^* \sqrt{\alpha}\mathbf{h}x|^2 | \mathbf{h}]}{\mathbb{E}[|\mathbf{w}^* \mathbf{n}|^2]} \quad (8)$$

$$= \frac{\alpha P}{\sigma^2} \|\mathbf{h}\|^2. \quad (9)$$

Since $\mathbf{h} \sim \mathcal{N}_C(\mathbf{0}, \mathbf{C})$ with \mathbf{C} a rank-1 covariance matrix, the above SNR is exponentially distributed. Recalling (1) and (5), its average value is given by

$$\text{SNR}_{\text{avg}} = \frac{\alpha P}{\sigma^2} \mathbb{E}[\|\mathbf{h}\|^2] \quad (10)$$

$$= \frac{\alpha P}{\sigma^2} \mathbb{E}[\text{tr}(\mathbf{h}\mathbf{h}^*)] \quad (11)$$

$$= \frac{\alpha P}{\sigma^2} \text{tr}(\mathbf{C}) \quad (12)$$

$$= \frac{\alpha P}{\sigma^2} \text{tr}(\mathbf{H}\Psi\mathbf{C}_r\Psi^*\mathbf{H}^*) \quad (13)$$

$$= \frac{\alpha P}{\sigma^2} \text{tr}(\Psi\mathbf{C}_r\Psi^*\mathbf{H}^*\mathbf{H}) \quad (14)$$

$$= \frac{\alpha P}{\sigma^2} \text{tr}(\Psi\mathbf{C}_r\Psi^* \mathbf{a}_r \mathbf{a}_b^* \mathbf{a}_b \mathbf{a}_r^*) \quad (15)$$

$$= \frac{\alpha P}{\sigma^2} N_b \text{tr}(\Psi\mathbf{C}_r\Psi^* \mathbf{a}_r \mathbf{a}_r^*) \quad (16)$$

$$= \frac{\alpha P}{\sigma^2} N_b \text{tr}(\mathbf{a}_r^* \Psi\mathbf{C}_r\Psi^* \mathbf{a}_r) \quad (17)$$

$$= \frac{\alpha P}{\sigma^2} N_b \mathbf{a}_r^* \Psi\mathbf{C}_r\Psi^* \mathbf{a}_r \quad (18)$$

$$= \frac{\alpha P}{\sigma^2} N_b N_r \mathbf{v}^* \Psi\mathbf{C}_r\Psi^* \mathbf{v} \quad (19)$$

$$= \frac{\alpha P}{\sigma^2} N_b \underbrace{N_r \zeta}_{\text{RIS power gain}} \quad (20)$$

where in (19) and (20) we introduced, respectively,

$$\mathbf{v} = \frac{1}{\sqrt{N_r}} \mathbf{a}_r \quad (21)$$

and

$$\zeta = \mathbf{v}^* \Psi\mathbf{C}_r\Psi^* \mathbf{v} \quad (22)$$

$$= \psi \text{diag}(\mathbf{v}^*) \mathbf{C}_r \text{diag}(\mathbf{v}) \psi^*. \quad (23)$$

Within the average SNR in (20), the multiplier N_b corresponds to the gain of the BS receive array, which leaves the product $N_r \zeta$ as the power gain provided by the RIS. This gain is made up of two factors:

- N_r , which reflects the power captured by the RIS acting as a receiver and does not depend on the RIS phase shifts,
- ζ , which represents the beamforming gain provided by the RIS acting as a transmitter, incorporating the effect of the RIS phase shifts. One can view ζ as the average power gain relative to these phase shifts being random.

If the channel realizations to/from the RIS could be perfectly estimated, the RIS phase shifts could be instantaneously optimized yielding $\zeta = N_r$, for a RIS power gain $N_r \zeta$ that would altogether be quadratic in the number of RIS elements [12]. In a two-timescale system, however, the beamforming gain ζ behaves rather differently.

IV. TWO-TIMESCALE BEAMFORMING GAIN

The optimum phase shifts are those that maximize the beamforming gain, ζ . The optimization of the RIS phase shifts can thus be cast, recalling (23), as

$$\zeta = \max_{\psi: |\psi_m|=1 \forall m} \psi \text{diag}(\mathbf{v}^*) \mathbf{C}_r \text{diag}(\mathbf{v}) \psi^* \quad (24)$$

whose objective function is quadratic, but whose unit-magnitude constraints are not convex. This problem is addressed in [13] with an approximation guarantee, while [14] introduces a low-complexity alternative optimization approach. Sidestepping numerical optimization procedures, in this section insights are gleaned analytically.

For $N_r = 1$, trivially $\zeta = 1$ in a two-timescale system as it would be with instantaneously optimized phase shifts. For $N_r = 2$, however, the latter would double to $\zeta = 2$ while the former amounts, after a bit of algebra, to

$$\zeta = \max_{\psi_0, \psi_1: |\psi_0|=1, |\psi_1|=1} 1 + \operatorname{Re} \left\{ c_1 e^{-j(\psi_1 - \psi_0)} e^{j2\pi \frac{d \cos \theta}{\lambda_c}} \right\}, \quad (25)$$

which, by setting $\psi_1 - \psi_0 = \arg(c_1) + 2\pi d \cos \theta_r / \lambda_c$, returns

$$\zeta = 1 + |c_1|. \quad (26)$$

As C_r is nonsingular, $|c_1| < 1$ and thus the two-timescale beamforming gain satisfies $\zeta < 2$, falling short of its instantaneously optimized counterpart. In fact, the two-timescale beamforming gain is strictly sublinear in N_r for every N_r . This can be appreciated by relaxing the constraints in (24) to $\|\psi\| = \sqrt{N_r}$, whereby

$$\zeta \leq \max_{\psi: \|\psi\| = \sqrt{N_r}} \psi \operatorname{diag}(\mathbf{v}^*) C_r \operatorname{diag}(\mathbf{v}) \psi^* \quad (27)$$

$$= N_r \lambda_{\max}(\operatorname{diag}(\mathbf{v}^*) C_r \operatorname{diag}(\mathbf{v})), \quad (28)$$

where $\lambda_{\max}(\cdot)$ denotes the largest eigenvalue of a matrix, and (28) is achieved by the maximum-eigenvalue eigenvector of $\operatorname{diag}(\mathbf{v}^*) C_r \operatorname{diag}(\mathbf{v})$. Since $\sqrt{N_r} \operatorname{diag}(\mathbf{v}^*)$ is a unitary matrix, the above is tantamount to

$$\zeta \leq \lambda_{\max}(C_r) \quad (29)$$

$$< \operatorname{tr}(C_r) \quad (30)$$

$$= N_r, \quad (31)$$

with (30) following from the nonsingular condition of C_r .

If the RIS elements are uncorrelated, then $\lambda_{\max}(C_r) = 1$ and the above corroborates the stronger result that, as expected, there is no beamforming gain to be had in a two-timescale system without RIS element correlation. In the sequel, therefore, only situations in which the RIS elements do exhibit correlation are considered.

Owing to the structure of \mathbf{v} , which descends from (2), the (k, ℓ) th entry of $\operatorname{diag}(\mathbf{v}^*) C_r \operatorname{diag}(\mathbf{v})$ equals

$$[\operatorname{diag}(\mathbf{v}^*) C_r \operatorname{diag}(\mathbf{v})]_{k, \ell} = c_n \frac{e^{j2\pi n d \cos \theta_r / \lambda_c}}{N_r}, \quad (32)$$

where, recall, $n = k - \ell$. Thus, the Toeplitz structure of C_r is readily inherited by $\operatorname{diag}(\mathbf{v}^*) C_r \operatorname{diag}(\mathbf{v})$, whereby its maximum eigenvalue is upper bounded by $\sum_{n=-\infty}^{\infty} |c_n|$ [15], such that

$$\zeta \leq \sum_{n=-\infty}^{\infty} |c_n|. \quad (33)$$

The beamforming gain is thus sure to be curbed if the right-hand side of (33) is finite, which corresponds to C_r being a Wiener-class Toeplitz matrix. This, in turn, is guaranteed if

$$|c_n| = o\left(\frac{1}{|n|}\right), \quad (34)$$

which, as seen in Sec. V, is satisfied by a number of functions that have been shown to be a satisfactory fit for the PAS.

Irrespective of whether (34) holds, a precise assertion of how the beamforming gain behaves can be made asymptotically in the number of RIS elements. Indeed, for $N_r \rightarrow \infty$, numerical optimizations become unnecessary as (24) admits a closed-form solution. Under mild conditions satisfied by any well-behaved PAS, for growing N_r the eigenvectors of $\operatorname{diag}(\mathbf{v}^*) C_r \operatorname{diag}(\mathbf{v})$ converge, on account of the Toeplitz nature of this matrix, to Fourier vectors of the form [15]

$$\frac{1}{\sqrt{N_r}} \left[1, e^{-j2\pi m/N_r}, \dots, e^{-j2\pi m(N_r-1)/N_r} \right]^* \quad (35)$$

for $m = 0, \dots, N_r - 1$. As these vectors (scaled by N_r) comply with the constraints in (24), the solution to this original problem is sure to equal that of the relaxed problem in (29), meaning that the optimum beamforming gain satisfies

$$\zeta \approx \lambda_{\max}(C_r), \quad (36)$$

which sharpens with growing N_r and becomes exact asymptotically. The RIS phase shifts achieving this beamforming gain, in turn, converge to the Fourier eigenvector (scaled by $\sqrt{N_r}$) associated with the maximum eigenvalue of C_r . As seen next, for many PAS functions of interest this eigenvalue is bounded from above.

V. EXAMPLES

Let us next entertain some of the functions most commonly considered to model the PAS.

- **Truncated Gaussian.** A Gaussian function with mean μ_θ and angular spread $\sigma_\theta > 0$, whose support is restricted to $\theta \in (0, \pi)$, has been shown to offer a good fit to the empirical PAS in elevated BSs [16]. The function is

$$\mathcal{P}(\theta) = \frac{K_G}{\sqrt{2}\sigma_\theta} \exp\left(-\frac{(\theta - \mu_\theta)^2}{2\sigma_\theta^2}\right), \quad (37)$$

where

$$K_G = \frac{1}{\sqrt{\pi}[1 - 2Q(\frac{\pi}{2\sigma_\theta})]}, \quad (38)$$

is a normalization factor ensuring that the PAS integrates to one, and $Q(\cdot)$ is the Gaussian Q-function.

For small σ_θ , the integration in (3) yields [10, Ch. 3]

$$|c_n| \approx \exp\left(-2 \left[\frac{\pi d n \sin(\mu_\theta) \sigma_\theta}{\lambda_c} \right]^2\right), \quad (39)$$

whereby (33) specializes to [17, Ch. 16.27]

$$\zeta \leq \vartheta\left(0, e^{-2 \left[\frac{\pi d \sin(\mu_\theta) \sigma_\theta}{\lambda_c} \right]^2}\right), \quad (40)$$

where $\vartheta(\cdot, \cdot)$ is the Jacobi theta function. The decay of (39) is decidedly faster than $1/|n|$ and the beamforming gain is therefore curbed.

- **Truncated Laplacian.** Extensive measurements have shown a strong fit of the Laplacian PAS, with a properly tuned σ_θ and support on $(0, \pi)$, to both indoor [18] and outdoor environments [19]. This function is [10, Ch. 3]

$$\mathcal{P}(\theta) = \frac{K_L}{\sqrt{2}\sigma_\theta} \exp\left(-\left|\frac{\sqrt{2}(\theta - \mu_\theta)}{\sigma_\theta}\right|\right), \quad (41)$$

with

$$K_L = \frac{1}{1 - \exp\left(-\frac{\pi}{\sqrt{2}\sigma_\theta}\right)}. \quad (42)$$

For small σ_θ , it holds that [20]

$$|c_n| \approx \frac{1}{1 + 2(\pi d n \sin(\mu_\theta) \sigma_\theta / \lambda_c)^2} \quad (43)$$

and, from

$$\pi \cot(\pi z) = \frac{1}{z} + 2z \sum_{n=1}^{\infty} \frac{1}{z^2 - n^2}, \quad (44)$$

it follows that (33) specializes to

$$\zeta \leq \frac{\lambda_c}{\sqrt{2}d \sin(\mu_\theta) \sigma_\theta} \coth\left(\frac{\lambda_c}{\sqrt{2}d \sin(\mu_\theta) \sigma_\theta}\right). \quad (45)$$

In this case, $|c_n| = \mathcal{O}(1/|n|^2)$, whereby the beamforming gain is again curbed.

- **Exponential correlation model.** This simpler model is

$$|c_n| = \kappa^{|n|}, \quad (46)$$

where $\kappa < 1$ is a parameter [21]. Leveraging the properties of the geometric series, (33) specializes to

$$\zeta \leq \frac{1 + |\kappa|}{1 - |\kappa|}, \quad (47)$$

which is always bounded.

The beamforming gain for the truncated Gaussian and Laplacian PAS functions is exemplified in Fig. 1 as a function of the number of RIS elements, with representative angular spreads and numerically computed RIS phase shifts. The dashed lines indicate the upper bounds to the beamforming gains, for those cases in which expressions are available; these upper bounds are seen to be tight, and they are approached rapidly as N_r grows large. Also included in the figure is the beamforming gain obtainable with instantaneously optimized RIS phase shifts, i.e., $\max_{\Psi} \mathbb{E}[v^* \Psi \mathbf{h}_r \mathbf{h}_r^* \Psi^* v]$; this gain grows linearly and sustainedly with N_r .

To complement the above, Fig. 2 depicts the beamforming gain as a function of the angular spread, with $N_r = 100$ as a proxy for $N_r \rightarrow \infty$. Not only is the gain curbed, but it is restricted to values that are modest and that decay rapidly. Unless $\sigma_\theta < 10^\circ$, we have that $\zeta < 8$ dB for both the Gaussian and the Laplacian PAS, no matter how large the RIS may be. For $\sigma_\theta \rightarrow 0$, the MS-RIS channel becomes line-of-sight

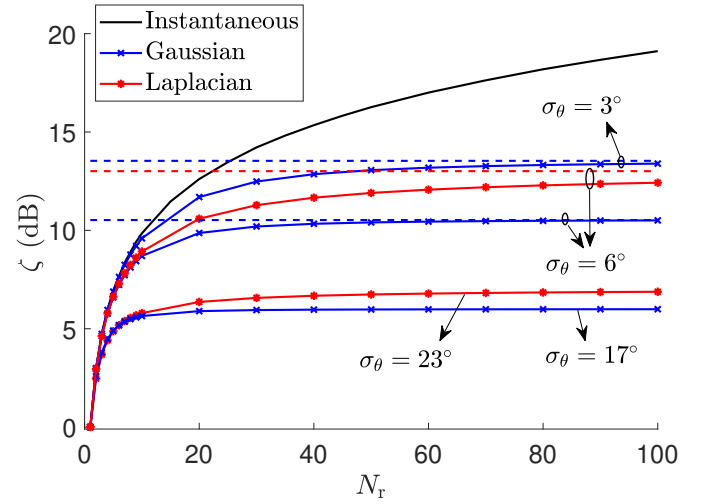


Fig. 1. Beamforming gain as a function of the number of RIS elements for different PASs, with the RIS element spacing set to $d = \lambda_c/2$. For the truncated Gaussian PAS, $\mu_\theta = \pi/4$ and $\sigma_\theta = \{3^\circ, 6^\circ, 17^\circ\}$ [16]. For the truncated Laplacian PAS, $\mu_\theta = \pi/4$ and $\sigma_\theta = \{6^\circ, 23^\circ\}$ [18, 20]. Included as benchmark is the gain with instantaneously optimized phase shifts.

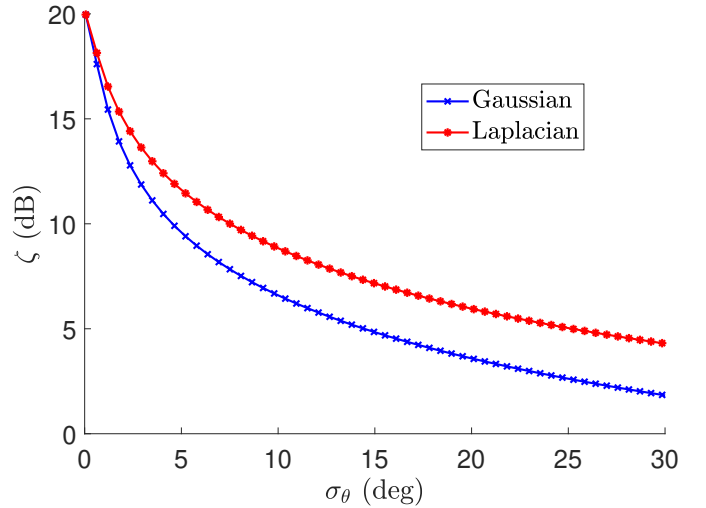


Fig. 2. Beamforming gain as a function of the angular spread for truncated Gaussian and Laplacian PAS, with $N_r = 100$, $\mu_\theta = \pi/2$, and $d = \lambda_c/2$.

and \mathbf{C}_r becomes rank-1, whereby the beamforming gain grows unboundedly with the number of RIS elements.

The average SNRs corresponding to some of the curves in Fig. 1 are depicted in Fig. 3. As the number of RIS elements increases, instantaneous phase-shift tuning delivers a quadratic improvement with N_r while, in the two-timescale examples, the asymptotic improvement is merely linear. Also noteworthy in the two-timescale examples is that the SNRs with the RIS phase shifts optimized numerically as per [11] are barely distinguishable from those with the asymptotically optimum Fourier values in (35). This excellent match indicates that the Fourier phase shifts, of lower computational complexity, are an enticing solution to configure a two-timescale linear RIS even for small N_r .

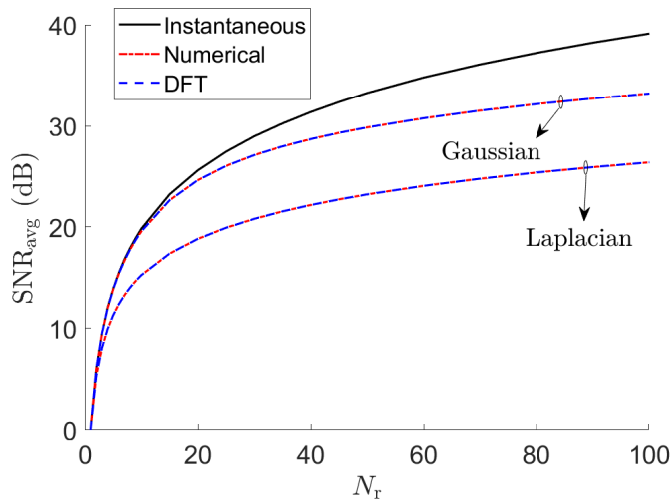


Fig. 3. Average SNR versus N_r with $N_b = 10$, $\theta_r = 80^\circ$, $\mu_\theta = \pi/4$, and $\alpha P/\sigma^2 = -10$ dB. For the truncated Gaussian PAS, $\sigma_\theta = 3^\circ$ [16]. For the truncated Laplacian PAS, $\sigma_\theta = 23^\circ$ [18]. Results shown for phase shifts computed numerically and for their asymptotic DFT values. Included as benchmark is the gain with instantaneously optimized phase shifts.

VI. CONCLUSION

The two-timescale approach to RIS-assisted communication avoids the costly estimation of the channels to/from the RIS. Moreover, computationally attractive Fourier phase shifts can be applied in the case of a linear RIS. This overall convenience, however, comes at a price in performance. The power gain, quadratic in the number of RIS elements if the RIS phase shifts could be instantaneously optimized, reverts to a scaling that is always sub-quadratic; for a broad class of channels, in fact, this scaling becomes merely linear beyond a relatively small number of elements. This poorer scaling with the number of elements curtails the ability of the RIS to provide a decisive advantage relative to ambient propagation [22, 23], and renders the RIS less competitive against alternatives such as relays and network-controlled repeaters [24]. The generalization of these findings to planar RIS entails dealing with block-Toeplitz covariance matrices. The results are qualitatively similar, but a larger number of RIS elements is required for the power gain scaling to become merely linear.

ACKNOWLEDGMENT

Work supported by the Horizon 2020 MSCA-ITN-METAWIRELESS Grant Agreement 956256, by MICIU under grant CEX2021001195-M, by ICREA, and by the Swedish SSF project SAICOM Grant No: FUS21-0004.

REFERENCES

- [1] Z. Huang *et al.*, “Intelligent surfaces aided high-mobility communications: Opportunities and design issues,” *IEEE Commun. Mag.*, vol. 62, no. 6, pp. 122–128, 2024.
- [2] L. Dai *et al.*, “Reconfigurable intelligent surface-based wireless communications: Antenna design, prototyping, and experimental results,” *IEEE Access*, vol. 8, pp. 45 913–45 923, 2020.
- [3] W. Tang *et al.*, “Wireless communications with reconfigurable intelligent surface: Path loss modeling and experimental measurement,” *IEEE Trans. Wireless Commun.*, vol. 20, no. 1, pp. 421–439, 2021.
- [4] W.-X. Long *et al.*, “Channel estimation in RIS-aided communications with interference,” *IEEE Wireless Commun. Letters*, vol. 12, no. 10, pp. 1751–1755, 2023.
- [5] Q. Li *et al.*, “Low-overhead channel estimation for RIS-aided multi-cell networks in the presence of phase quantization errors,” *IEEE Trans. Veh. Technol.*, vol. 73, no. 5, pp. 6626–6641, 2024.
- [6] K. Zhi *et al.*, “Two-timescale design for reconfigurable intelligent surface-aided massive MIMO systems with imperfect CSI,” *IEEE Trans. Inf. Theory*, vol. 69, no. 5, pp. 3001–3033, 2022.
- [7] Q. Peng *et al.*, “Two-timescale design for reconfigurable intelligent surface-aided URLLC,” *IEEE Trans. Wireless Commun.*, pp. 1–1, 2024.
- [8] Y. Han *et al.*, “Large intelligent surface-assisted wireless communication exploiting statistical CSI,” *IEEE Trans. Veh. Technol.*, vol. 68, no. 8, pp. 8238–8242, 2019.
- [9] A. Kammoun *et al.*, “Asymptotic max-min SINR analysis of reconfigurable intelligent surface assisted MISO systems,” *IEEE Trans. Wireless Commun.*, vol. 19, no. 12, pp. 7748–7764, 2020.
- [10] R. W. Heath Jr and A. Lozano, *Foundations of MIMO Communication*. Cambridge, U.K.: Cambridge Univ. Press, 2019.
- [11] M. Sadeghian *et al.*, “Pilot-to-data power ratio in RIS-assisted multi-antenna communication,” *IEEE Wireless Commun. Letters*, pp. 1–1, 2025.
- [12] Q. Wu and R. Zhang, “Intelligent reflecting surface enhanced wireless network via joint active and passive beamforming,” *IEEE Trans. Wireless Commun.*, vol. 18, no. 11, pp. 5394–5409, 2019.
- [13] A. M.-C. So *et al.*, “On approximating complex quadratic optimization problems via semidefinite programming relaxations,” *Math. Program.*, vol. 110, no. 1, pp. 93–110, 2007.
- [14] A. Sirojuddin *et al.*, “Low-complexity sum-capacity maximization for intelligent reflecting surface-aided MIMO systems,” *IEEE Wireless Commun. Letters*, vol. 11, no. 7, pp. 1354–1358, 2022.
- [15] R. M. Gray *et al.*, “Toeplitz and circulant matrices: A review,” *Found. Trends Commun. Inform. Theory*, vol. 2, no. 3, pp. 155–239, 2006.
- [16] T.-S. Chu and L. Greenstein, “A semi-empirical representation of antenna diversity gain at cellular and PCS base stations,” *IEEE Trans. Commun.*, vol. 45, no. 6, pp. 644–646, 1997.
- [17] M. Abramowitz and I. A. Stegun, *Handbook of mathematical functions with formulas, graphs, and mathematical tables*. Dover Publications, 1964.
- [18] Q. Spencer *et al.*, “Modeling the statistical time and angle of arrival characteristics of an indoor multipath channel,” *IEEE J. Sel. Areas Commun.*, vol. 18, no. 3, pp. 347–360, 2000.
- [19] K. Pedersen *et al.*, “A stochastic model of the temporal and azimuthal dispersion seen at the base station in outdoor propagation environments,” *IEEE Trans. Veh. Technol.*, vol. 49, no. 2, pp. 437–447, 2000.
- [20] A. Forenza *et al.*, “Simplified spatial correlation models for clustered MIMO channels with different array configurations,” *IEEE Trans. Veh. Technol.*, vol. 56, no. 4, pp. 1924–1934, 2007.
- [21] S. Loyka, “Channel capacity of MIMO architecture using the exponential correlation matrix,” *IEEE Commun. Letters*, vol. 5, no. 9, pp. 369–371, 2001.
- [22] M. Sadeghian *et al.*, “RIS in indoor environments: Benchmarking against ambient propagation,” *Asilomar Conf. Signals, Systems, and Computers*, pp. 127–133, 2023.
- [23] D. Chizhik *et al.*, “Comparing power scattered by RIS with natural scatter around urban corners,” *IEEE Int. Symp. Antennas Propag. USNC-URSI Radio Science Meeting*, 2022.
- [24] E. Björnson *et al.*, “Intelligent reflecting surface versus decode-and-forward: How large surfaces are needed to beat relaying?” *IEEE Wireless Commun. Letters*, vol. 9, no. 2, pp. 244–248, 2020.